Robust circuit design for optical sensing based on multi-wavelength waveguide holograms

D. De Vocht, Y. Jiao, and E.A.J.M. Bente

Photonic Integration Group, Department of Electrical Engineering, Eindhoven University of Technology, PO Box 513, 5600 MB Eindhoven, The Netherlands.

d.j.y.d.vocht@tue.nl

Abstract

We present a photonic integrated circuit design for metrology or gas sensing that can withstand several fabrication-induced variations or experimental misalignments. Featuring the largest waveguide hologram on a high refractive index platform, our design directs light from three on-chip waveguides (tuned to wavelengths of 1300 nm, 1450 nm and 1600 nm) to a 30 µm spot on a mirror positioned 10 mm above the chip's surface. A receiving waveguide hologram then couples the reflected light back into the chip. Our semi-analytical model reveals that the 3 dB points in power transmission with variation in effective refractive index and misalignment errors occur at approximately 0.002 and 0.1°, respectively. The latter is significantly higher than the tilt accuracy of standard mirror mounts, rendering losses due to mirror misalignments negligible. To ensure robustness to fabrication-induced variations in the effective refractive index, we position the holograms adjacent to each other, ensuring they encounter identical refractive index changes and maintain similar emitting/receiving angles. This allows for straightforward compensation through minor adjustments to the mirror angle or input wavelengths. Our design method paves the way for the miniaturization of optical sensors, allowing the creation of compact, robust optical sensor systems that perform reliably even in the presence of fabrication variations.

Introduction

Monolithically integrating a chip-to-free-space coupler on a photonic integrated circuit enables further miniaturization of optical devices by reducing the need for external optics such as lenses or gratings. Various designs are proposed for integrated receivers or emitters containing grating couplers [1], waveguide holograms [2] or metalenses [3]. Kim et al [4] achieved monolithic integration of a single-wavelength emitter and receiver on a single chip, converting light to a mirror positioned 4 mm above the chip's surface. However, due to fabrication defects, their device encountered beam misalignments, leading to a reduced coupling efficiency of up to -3.5 dB.

To address these challenges, we present a robust circuit design for optical sensing that can withstand several fabrication-induced variations and experimental misalignments. As

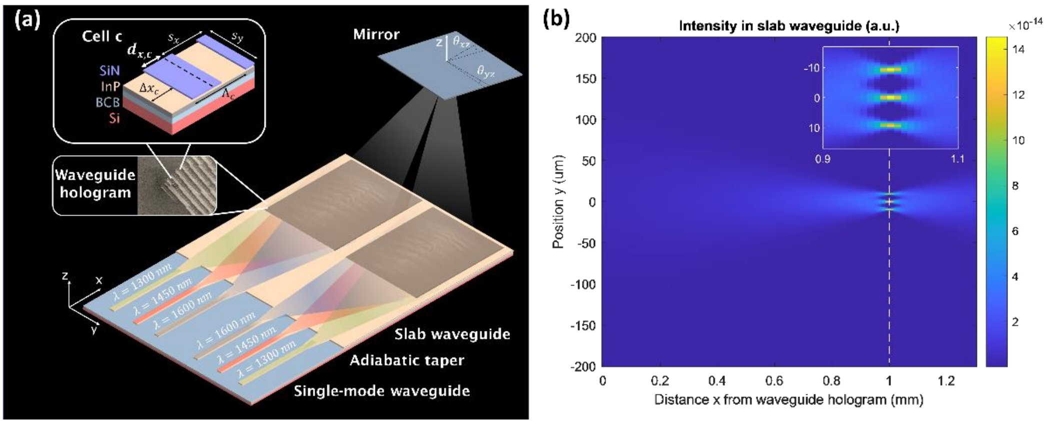

Figure 1 (a) Schematic of our integrated coupling circuit providing an overview of key design parameters for the waveguide holograms. (b) Simulated intensity profile in the slab waveguide (top view) of the receiver summated for the three wavelengths. The dashed line indicates the end of the slab region. The inset offers a closer look at the focused spot at the receiving taper.

illustrated in Figure 1(a), our emitter and receiver make the light propagate from three single-mode waveguides - each designed for wavelengths of 1300 nm, 1450 nm and 1600 nm, respectively - to a mirror in free space. This process involves a taper for initial mode expansion, a slab waveguide for further expansion, and a waveguide hologram to emit and focus the light into a narrow Gaussian beam on the mirror surface. The waveguide holograms, sized at 446 µm × 446 µm, stand as the largest ever published waveguide hologram design on a high refractive index platform. This substantial size is essential for creating a 30 µm focal spot on the mirror positioned 10 mm above the chip's surface. We have designed the waveguide holograms using our recently developed semi-analytical model [5], [6]. Table 1 gives an overview of our circuit's design parameters. Figure 1(b) shows how the multi-wavelength receiver couples the light towards the narrow tapers located 1 mm away from the waveguide hologram.

In this paper, we will rigorously investigate our circuit's performance under conditions of effective refractive index errors and mirror misalignment. This has led to deeper insights and led to positioning the emitter and receiver adjacent to each other. To keep it concise, we confine our study to the wavelength of 1450 nm.

Effective refractive index variations

An effective refractive index n_{eff} describes the propagation of the guided mode within the slab waveguide or waveguide hologram. We assume n_{eff} linearly depends on the filling ratio fr in the waveguide hologram

$$n_{eff} = fr\, n_{eff,SiN} + (1 - fr\,)n_{eff,etched} \qquad (1)$$

with $n_{eff,SiN}$ (and $n_{eff,etched}$) the effective refractive index when (not) including the Si_3N_4 layer (see insert Figure 1(a)). Variations in the effective refractive index Δn_{eff} can be caused by discrepancies in the thicknesses of the waveguide layer and the Si_3N_4 layer, over/under-etching of nanostructures during fabrication, or potential inaccuracies in n_{eff} modelling used. We consider the variations $\Delta n_{eff,SiN}$ and Δn_{eff}, where $\Delta n_{eff,SiN} = \frac{1}{fr}\Delta n_{eff}$ as evident from Eq. (1), and this perturbation is confined to the hologram region. We utilize our semi-analytical model to assess the impact of these errors on the received intensity profile in the slab waveguides. Figure 2(a-c) shows that apart from a noticeable decay in peak intensity, the profile remains similar for the different $\Delta n_{eff,SiN}$ and Δn_{eff}. We notice that the focal spot shifts up to 4 µm when $\Delta n_{eff} \leq 0.005$. Given the mean value of the filling ratio fr in the waveguide hologram is around 26 %, the peak intensity decay is more pronounced for Δn_{eff} than $\Delta n_{eff,SiN}$. Since the waveguide layers are epitaxially created and the Si_3N_4 is deposited using Plasma Enhanced Chemical Vapor Deposition (PECVD), $\Delta n_{eff,SiN}$ is likely larger than Δn_{eff}. The 3 dB point occurs at $\Delta n_{eff,SiN}$ =0.0021 and Δn_{eff} =0.0071. To explain the cause of this decay, we consider the common assumption for waveguide holograms that each of the nanostructures locally acts as an independent grating coupler. So, we apply the grating equation

$$\sin\theta_{xz} = n_{eff} - \lambda_0/\Lambda_x \qquad (2)$$

with θ_{xz} the emittance/receiving angle of the waveguide hologram, λ_0 the wavelength and Λ_x the pitch between two neighbouring nanostructures. Consequently, if n_{eff} varies with 0.002 (0.07 % of its nominal value), θ_{xz} varies with 0.11° (2.2 % of its nominal value). To ensure the emitter and receiver encounter identical refractive index changes

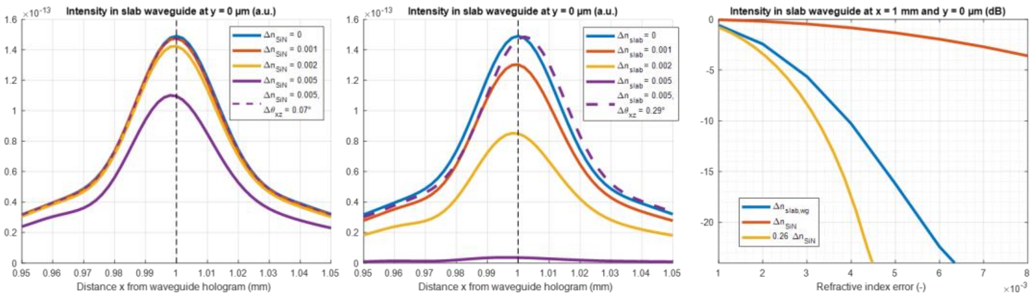

Figure 2 Impact of effective refractive index variations on the coupling to the receiver. Intensity profile in the slab waveguide of the receiving coupler in case of effective refractive index errors due to a mismatch in (a) the SiN or (b) underlying waveguide layers. The purple dotted line represents the case when the mirror is readjusted to compensate for these errors. (c) Intensity decay due to the effective refractive index errors.

and maintain similar emitting/receiving angles, we position the holograms adjacent to each other (Fig. 1(a)). As depicted in Eq. (2) and Fig. 2(a-b), we can compensate for refractive index errors by tilting the mirror's angle by less than 0.29°. Alternatively, if the application allows, we can tune the wavelength by less than 2.9 nm.

Mirror misalignment

As discussed earlier, we identified the relationship between θ_{xz} and n_{eff}. We conclude that the 3 dB point for mirror misalignments in the xz-plane occurs at $\Delta\theta_{xz} = 0.11°$. Given the sufficiently small cell pitch s_y, diffraction effects are negligible in the yz plane. Consequently, small mirror misalignments in the yz plane, denoted by $\Delta\theta_{yz}$, minimally impact the coupling efficiency. For $\Delta\theta_{yz} = \pm 0.1°$, the centre of the received beam at the waveguide hologram displaces by $\Delta y = \pm 18\ \mu m$. Since the waveguide hologram acts as a lens in the slab waveguide this shift does not displace the focal spot. However, $\Delta\theta_{yz}$ induces a reorientation of the waveguide vector inside the waveguide hologram, leading to a lateral shift of the focal spot. This shift diminishes the overlap between the received intensity and the mode profile of the taper, thereby reducing the coupling efficiency. In Figure 3(a-b), we visualize the impact of $\Delta\theta_{yz}$ on the intensity profile and the overlap integral with the taper's mode profile. We notice the focal spot shifts 7.6 µm per 1° change in θ_{yz}. The 3 dB point is at $\Delta\theta_{yz} = 0.13°$. Overetching can introduce variations in the taper end width. To enhance the robustness of our design, we can widen the taper by 50 %, incurring only a 6 % drop in intensity in the nominal case. This adjustment simultaneously mitigates sensitivity to overlay errors between the lithography step of the

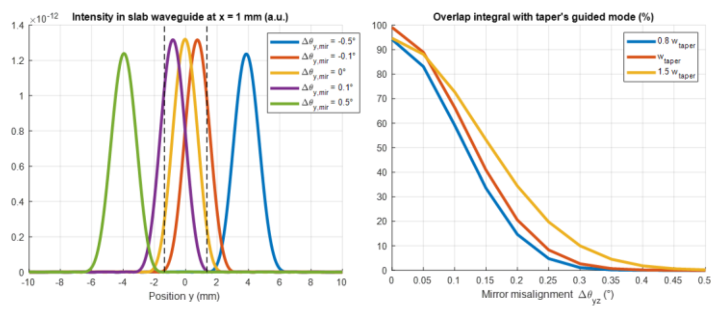

Figure 3 Impact of mirror misalignments in the yz-plane on the coupling to the receiver. (a) Intensity profile at the receiving taper for different mirror misalignments. (b) Overlap integral between the received intensity profile and the taper's mode profile in case of different mirror misalignments and taper widths.

taper and the waveguide hologram. Notably, the tilt adjustment sensitivity of typical good quality mirror mounts (100 TPI actuator in a mount for 1-inch mirror) equals 0.001 °, two orders of magnitude lower than the errors we notice here.

Table 1 Design parameters of our circuit and waveguide hologram

Wavelength	**1300 nm**	**1450 nm**	**1600 nm**
Width Ridge waveguide		400 nm	
Width taper end	1.0 µm	1.2 µm	1.4 µm
Y position taper	-9.3 µm	0 µm	9.3 µm
Length slab waveguide		1000 µm	
Length/Width CGWH		446 µm	
Pitch cell s_x		536 nm	
Pitch cell s_y		350 nm	
$n_{eff,SiN}$	2.894	2.812	2.742
$n_{eff,unetched}$	2.8717	2.785	2.710
Mirror location z		10 mm	
Mirror orientation		$\theta_{xz} = 5°$ and $\theta_{yz} = 0°$	
Target spot diameter		30.6 µm	

Conclusion

Our simulations quantify the robustness of our proposed photonics integrated circuit design for multi-wavelength chip-to-free-space coupling. By positioning the emitter and receiver adjacent to each other, our design minimizes the impact of fabrication-induced variations in the effective refractive index. We even demonstrate the capability of compensating for these variations through minor adjustments in the mirror's angle or input wavelengths. Additionally, we conclude that considering the precision of good quality mirror mounts, losses due to mirror tilts can be easily avoided. We are currently preparing experiments to validate the robustness of our design.

Acknowledgements

This publication is part of the project FreeSense with project number 17971 of the research program HTSM which is financed by the Dutch Research Council (NWO). We thank Professor Irwan Setija for the insightful discussions.

References

[1] L. Cheng, S. Mao, Z. Li, Y. Han, and H. Y. Fu, "Grating Couplers on Silicon Photonics: Design Principles, Emerging Trends and Practical Issues," *Micromachines 2020, Vol. 11, Page 666*.

[2] J. Cheng, D. Ansari-Oghol-Beig, and H. Mosallaei, "Wave manipulation with designer dielectric metasurfaces," *Opt Lett*, vol. 39, no. 21, p. 6285, Nov. 2014.

[3] A. Yulaev *et al.*, "Metasurface-Integrated Photonic Platform for Versatile Free-Space Beam Projection with Polarization Control," *ACS Photonics*, vol. 6, no. 11, pp. 2902–2909, Nov. 2019.

[4] S. Kim *et al.*, "Photonic waveguide to free-space Gaussian beam extreme mode converter," *Science & Applications*, 2018.

[5] D. De Vocht, T. Liu, Y. Jiao, and E. Bente, "Experimental Validation of a Far-Field Emission Model of Computer-Generated Waveguide Holograms," in *Optica Advanced Photonics Congress 2023*, 2023, p. JTu4A.10.

[6] D. De Vocht, I. Setija, Y. Jiao, and E. Bente, "Design of Controlled 2D Intensity Profile of Output Beam from Multi-Wavelength Waveguide Hologram," in *Frontiers in Optics Conference*, 2023, p. JTu4A.84.